

Multi-Dimension Scaling as an exploratory tool in the analysis of an immersed membrane bioreactor

A. Bick^{1,2*}, F. Yang³, S. Shandalov³, A. Raveh⁴ and G. Oron^{3,5,6}

¹*Department of Industrial Engineering and Management, Jerusalem College of Technology,
21 Havaad Haleumi St., Jerusalem, 91160 Israel*

²*Department of Chemical Engineering, Shenkar College of Engineering and Design,
12 Anna Frank street, Ramat Gan, 52526, Israel*

³*J. Blaustein Institutes for Desert Research, Ben-Gurion University of the Negev,
Kiryat Sde Boker, 84990, Israel*

⁴*The school of business administration, The Hebrew University, Jerusalem, Israel*

⁵*Department of Industrial Engineering and Management, and the program for Environmental Engineering,
Ben-Gurion University of the Negev, Beer Sheva, 84105, Israel*

⁶*The Grand Water Research Institute, Technion, Haifa, 32000, Israel*

(Received December 21, 2009, Accepted October 15, 2010)

Abstract. This study presents the tests of an Immersed Membrane BioReactor (IMBR) equipped with a draft tube and focuses on the influence of hydrodynamic conditions on membrane fouling in a pilot-scale using a hollow fiber membrane module of ZW-10 under ambient conditions. In this system, the cross-flow velocities across the membrane surface were induced by a cylindrical draft-tube. The relationship between cross-flow velocity and aeration strength and the influence of the cross-flow on fouling rate (under various hydrodynamic conditions) were investigated using Multi-Dimension Scaling (MDS) analysis. MDS technique is especially suitable for samples with many variables and has relatively few observations, as the data about Membrane Bio-Reactor (MBR) often is. Observations and variables are analyzed simultaneously. According to the results, a specialized form of MDS, CoPlot enables presentation of the results in a two dimensional space and when plotting variables ratio (output/input) rather than original data the efficient units can be visualized clearly. The results indicate that: (i) aeration plays an important role in IMBR performance; (ii) implementing the MDS approach with reference to the variables ratio is consequently useful to characterize performance changes for data classification.

Keywords: aeration; cross-flow velocity; draft tube; Immersed membrane bioreactor; membrane fouling; multi-dimension analysis.

1. Introduction

The scarcity of water resources in arid and semi-arid areas of the world, especially in the Middle East region, has changed public attitude towards wastewater management. Adequate management of wastewater is now a necessity and not an option (Sopponsiri *et al.* 2004, Rieger *et al.* 2005, Macedonio *et al.* 2006, Koning *et al.* 2008, Salgot 2008).

Membrane BioReactor (MBR) in which the membrane separation process is combined with biological processes is an efficient alternative for wastewater treatment and reuse (Drews *et al.* 2006, Lesjean and Leiknes 2006, Wenbo *et al.* 2006, Choi *et al.* 2008, Oron *et al.* 2008, Sridang *et al.* 2008). The MBR

* Corresponding author, Dr., E-mail: gidi@bgu.ac.il

presents many advantages over conventional processes due to its high organic loading rate, improved effluent quality, small footprint and low surplus sludge production (Bick *et al.* 2005, Qin *et al.* 2007, Abegglen *et al.* 2008, Chang *et al.* 2008). However, the major process problem with MBRs is the membrane fouling due to the physicochemical interactions between the membrane material and the components in the mixed liquor (Pollice *et al.* 2005, Le-Clech *et al.* 2006, Mosqueda-Jimenez *et al.* 2006, Petala *et al.* 2006, Shon *et al.* 2006, McAdam *et al.* 2007, Shon *et al.* 2008, Matos *et al.* 2008, Tan *et al.* 2008, Beyer *et al.* 2010). Fouling results in a permeate flux decrease or Trans-Membrane Pressure (TMP) increases over time when the process is operated under constant TMP or constant flux conditions, respectively. Along with the fouling, membrane permeability decreases and energy demand increases (Song *et al.* 2004, Chae *et al.* 2006, Bick *et al.* 2007).

In immersed MBR (IMBR), hydrodynamic characteristics, which fluctuate with various operating conditions, play an important role concerning membrane fouling and system performance. A crossflow, induced by air bubbles rising from a diffuser below the membrane modules, creates shear stress and generates a mass back-transport of the deposited particles along the membrane surface. The crossflow has proved it's efficiency for minimizing membrane fouling (Jiang *et al.* 2003, Gillerman *et al.* 2006).

The purpose of this study is threefold: (i) to investigate the membrane fouling rate under different operating conditions, (ii) to optimize the performance of an IMBR system which was equipped with a hollow fiber membrane module and a draft tube, and; (iii) to estimate the application of operational research tool of Multi-Dimension Scaling (MDS) analysis for performance analysis: a methodology for presenting data graphically. Results from the first stage of operation of the IMBR are thus presented.

2. Materials and methods

2.1 Management modeling

Management modeling provides effective means of rapidly testing and evaluating different scenarios for a given system operated under diverse conditions (Chen *et al.* 2005, Rossi *et al.* 2005, Jiang *et al.* 2007, Oehmen *et al.* 2007, Bick *et al.* 2009, Chen *et al.* 2010). Well-defined models allow examination of diverse hypothetical situations, which yield perceptive insight into the analyzed phenomena. The various aspects of IMBR can be viewed at the following levels: (i) the local level of the isolated process: economic, chemical, microbial and membrane performance criteria (Cicek *et al.* 2002, Joss *et al.* 2005, Joss *et al.* 2006, Abegglen *et al.* 2008, Agashichev 2009, Yang *et al.* 2009), and; (ii) at the regional level of water sources utilization, which includes membrane technology issues (Salgot 2008, Bottino *et al.* 2009). At this level, IMBR performance is only one link in a multi-component system. Other phases to be considered in management modeling include environmental considerations, disposal of concentrates, treatment efficiencies, regulatory and risk issues (Leiknes and Ødegaard 2007, Winward *et al.* 2008).

2.2 Multi-Dimension Scaling (MDS) and CoPlot

The Technical Efficiency (TE) of a system can be defined as the ratio r_{op} between outputs of the system and inputs where it is imperative to consider multiple inputs and outputs (Charnes *et al.* 1978).

$$r_{op} = \frac{\text{Output}_o}{\text{Input}_p} \quad \forall o, p = 1, 2, 3.. \quad (1)$$

This method differs from other decision supporting methods and it does not focus on the complete data set, but rather on individual Decision-Making Units (DMU). These DMU use a variety of identical inputs to produce a variety of identical outputs. It can be assumed that there is data available for n DMUs' (IMBR test records). Essentially, the higher the ratio (r_{op}) a unit receives, the more efficient the DMU is considered over that specific attribute (Charnes *et al.* 1978).

Many research questions dealing with TE require the analysis of complex multivariate data. Briefly, most multivariate approaches can be broadly classified as dependence methods (*e.g.*, multiple regression, discriminant analysis, multivariate analysis of variance) that are typically used to evaluate the association between dependent and independent variables or as interdependence methods (*e.g.*, principal component analysis, factor analysis, cluster analysis) that are typically used to evaluate the mutual association among all variables with no distinction made among the variable types (Schilli *et al.* 2010). One interdependence method, multidimensional scaling (MDS), facilitates the analysis of multivariate data by reducing multidimensional data into a two-dimensional structure that attempts to uncover the 'hidden structure' in a data set by creating a pictorial representation of the data. The MDS map graphically represents the proximities (or similarities) between objects (*i.e.*, observations or events). Similarities between the observations in the data set are transformed into distances on a map such that similar observations are closer together than less similar observations.

In this way, a single picture illustrates the relationships among all the observations. MDS, initially developed in the 1960s, has been used to evaluate the relationships among observations, to identify clusters of similar observations, and to find outliers (Raveh 2000). However, MDS maps have two key limitations: (i) MDS does not simultaneously map the variables and the observations, and; (ii) the MDS map has no orientation, thereby limiting the map's interpretability.

This paper describes an adaptation of MDS, called CoPlot that addresses both these limitations. CoPlot is a method for the graphical analysis of multivariate data that enables simultaneous analysis of observations and variables (hence, its name). Additionally, CoPlot maps the observations and variables in a manner that preserves their relationships, allowing richer interpretations of the data. Importantly, CoPlot allows analysis of a dataset where the number of variables is greater than the number of observations and CoPlot map could also be used to identify outliers and errors in the data, assessment of the relationships within the data, and for selection of key variables for subsequent analysis.

CoPlot has been used previously in economics to evaluate the performance of banks (Lipshitz and Raveh 1994, Adler and Raveh 2006), but has not been used in water treatment. In this paper, the utility of CoPlot is demonstrated for visual representations of multivariate MBR test data.

CoPlot's output is a visual display of its findings [Given an input matrix $Y_{n \times v}$ of v variable values for each of n observations (see for example Table 1)]. It is based on two graphs that are superimposed on each other (Bravata *et al.* 2008). The first graph maps the n observations into a two-dimensional space. This mapping, if it succeeds, conserves distance: observations that are close to each other in v dimensions and are also close in two dimensions, and vice versa. The second graph (Fig. 1) consists of v arrows, representing the variables, and shows the direction of the gradient along each one. Thus, CoPlot is an exploratory tool, which graphically represents: (i) correlation among the attributes using which the groupings are made, (ii) correlation among the units under observation, and; (iii) mutual relationship among the units and their measuring attributes (Sonicki *et al.* 2009).

The CoPlot analysis consists of four stages. The aim of the first stage is to normalize the variables, which is needed in order to be able to relate them to each other, although each has different units and scale. This is done in the usual way. In other words, the elements of the matrix Y_{ij} are scores

Table 1 A sample of IMBR pilot plant parameters (Air flow 5.1 m³/hr)

DMU (Decision making unit)	Input			Output	
	Accumulated operating hours	Temp. (°C)	Trans-membrane pressure (TMP) (bar)	Permeate flux (Liter/m ² -hr)	Fouling rate dP/dt (bar)
1	0.83	27.5	0.09	45.7	0.000
2	2.5	25.2	0.15	73.5	0.000
3	4	25.0	0.20	89.8	0.007
4	6.67	25.4	0.25	101.2	0.007
5	8.17	26.2	0.30	114.4	0.007
6	10.33	26.2	0.35	128.9	0.017
7	12.5	26.0	0.42	142.2	0.037
8	14.5	26.6	0.51	158.3	0.067

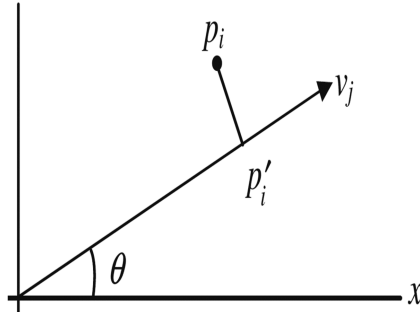


Fig. 1 CoPlot: Adding the variable vectors. The point p_i corresponds to the coordinates for observation $i = 1, \dots, n$. The vector v_j is for the variable $j = 1, \dots, m$. The x -axis is rotated through an angle θ to give a point p'_i , which is the projection of p_i onto the vector v_j . The correlation between the n new projected scores and the original n values for variable j are computed, and the choice for θ is the one that maximizes this correlation.

and the deviations from column means \bar{Y}_j , divided by their standard deviations (D_j), are normalized into Z_{ij} as follows

$$Z_{ij} := (Y_{ij} - \bar{Y}_j)/D_j \quad (2)$$

In the second stage, a measure of dissimilarity $S_{ik} \geq 0$ between each pair of observations (rows of $Z_n \times v$) is chosen and a symmetric $n \times n$ matrix is produced from all the different pairs of observations. To measure S_{ik} , the sum of absolute deviations (generally defined as city-block distance) as a measure of dissimilarity is used

$$S_{ik} = \sum_{j=1}^v |Z_{ij} - Z_{kj}| \quad (3)$$

In stage three, the matrix S_{ik} is mapped by means of a MDS method. Such an algorithm maps the matrix S_{ik} into an Euclidean space, of two dimensions in our case, such that “close” observations (with a small dissimilarity between them) are close to each other on the map, while “distant” ones are also distant on the map. Formally the requirement is as follows. Consider two observations, i and

k , that are mapped a distance of d_{ik} from each other. This distance has to reflect the dissimilarity S_{ik} (this is actually a relative measure), and the important constraints are: $S_{ik} < S_{lm}$ if $d_{ik} < d_{lm}$.

CoPlot procedure uses the Guttman's Smallest Space Analysis, or SSA (Guttman 1968, Raveh 2000). SSA uses the "coefficient of alienation", Θ as a measure of "goodness-of-fit". The intuition for Θ comes directly from the above MDS requirement: A success of fulfilling it implies that the product of the differences between the dissimilarity measures and the map distances are positive. In a normalized form, a new variable is defined as

$$\mu_{ca} = \frac{\sum_{i,k,l,m} (S_{ik} - S_{lm})(d_{ik} - d_{lm})}{\sum_{i,k,l,m} |S_{ik} - S_{lm}| |d_{ik} - d_{lm}|} \quad (4)$$

Thus μ_{ca} can attain the maximal value of 1 (Raveh 2000). This variable is used to define Θ as follows

$$\Theta = \sqrt{1 - \mu_{ca}^2} \quad (5)$$

The details of the SSA algorithm are beyond the scope of this paper, and were presented in the literature (Guttman 1968). It is a widely used method in social sciences, and several examples along with intuitive descriptions can be found (Raveh 2000). The outcome of this stage is a two-dimensional map of n observations and the CoPlot user can color code observations with any categorical variable that has up to 16 different values.

The map generated thus far is a classical MDS map without orientation or meaningful axes. In the fourth stage of the CoPlot method, v arrows are drawn on the Euclidean space obtained in the previous stage. Each variable j is represented by an arrow j , emerging from the center of gravity of the n points. The direction of each arrow is chosen so that the correlation between the actual values of the variable j and their projections on the arrow is maximal (the arrows' length is undefined). Therefore, observations with a high value in this variable should be in the part of the space the arrow points to, while observations with a low value in this variable will be at the other side of the map. The magnitude of the j maximal correlations measures the "goodness-of-fit" of the j regressions. Higher is the correlation, the better is the arrow representations of the variables and those having low correlations should be eliminated.

Moreover, arrows associated with highly correlated variables will point in about the same direction, and vice versa. As a result, the cosines of angles between these arrows are approximately proportional to the correlations between their associated variables (Raveh 2000).

The "goodness-of-fit" measure for each variable is obtained as follows: For each possible variable vector, CoPlot projects the points onto the vector, thereby yielding n projected values. These projected values can now be compared with the observed values. The axis that is chosen is the one that maximizes the correlation between the projected values and the observed values. Fig. 1 depicts how this is performed. The point p_i corresponds to the coordinates for observation $i = 1, \dots, n$. The vector v_j is for the variable $j = 1, \dots, m$. The x -axis is rotated through an angle θ to give a point p'_i , which is the projection of p_i onto the vector v_j . The correlation between the n new projected scores and the original n values for variable j are computed, and the choice for θ is the one that maximizes this correlation. Note that this maximization can be achieved numerically by calculating all 360° possibilities for θ . This calculation is performed separately for each variable vector.

These variable vectors have four useful properties. First, vectors for highly correlated variables point in the same direction, vectors for highly negatively correlated variables are oriented along the same axis but in opposing directions, and vectors for variables that are not correlated are orthogonal to each other. Second, each vector emanates from the center of gravity, which serves as the origin. An observation located at or near the origin is an average observation (it has an average value in all variables). Third, the length of each vector is proportional to the correlation (namely the “goodness of fit”) between the original data for that variable and the projections of the observations onto the vector. Finally, the angle between the vectors v_j and v_k is a reflection of the correlation between the j^{th} and k^{th} variables because the data are normalized, the cosine of the angle between the vectors is the correlation. Therefore, the researcher can study the correlational structure among the variables in a single graphical output (Raveh 2000).

In practical terms, the user imports data, selects variables and observations for inclusion in the analysis, creates the CoPlot map, evaluates “goodness-of-fit” parameters, selects the map to view (observations only, variables only, or both observations and variables), and then selects variables for color coding the observations for greater interpretation. Qualitative variables can be selected for color coding and may either be included in the computation of the map or can be excluded from the computation of the map but still used for color coding. For example, if a variable was found to have low “goodness-of-fit”, it might be excluded from the computation of the map but could still be used to color code variables to facilitate the interpretation of the data.

CoPlot produces two “goodness-of-fit measures”: one that describes how well the CoPlot map represents the observations and another that describes how well the CoPlot map represents the variables. The first “goodness-of-fit” measure is a “coefficient of alienation”, which indicates the relative loss of information that arises when the multidimensional data are transformed into two dimensions. The lower the value of the “coefficient of alienation”, the smaller the loss of information in the process of reducing the original data set to a two-dimensional map. In other words, the lower the “coefficient of alienation”, the more precise the representation of the MDS model to the proximities, and values below 0.15 are considered good (Guttman 1968).

In general, as the number of variables increases, the “coefficient of alienation” increases. The “coefficient of alienation” measures the discrepancy between every pair of points and the original matrix of “similarities” that comprises distances between points, so that this index provides a comparison between two matrices: The matrix similarities (which are “inputs”) and the matrix of the distances on the map (which are “outputs”) obtained by the algorithm. When these two matrices (inputs and outputs) are identical, the “coefficient of alienation” is zero (perfect).

The second “goodness-of-fit” measure is produced at the stage of calculating the correlation between the original data for each variable and the projection of each observation onto that vector in the CoPlot map. In general, the methodology maximizes the “correlations” (actually the normalized cross-products) of the vector of “inputs”, which are the actual distances from each point to every other point, and the “outputs”, which are the coordinates of the vectors that go into the map. Thus, the “goodness-of-fit” measures are the correlational measure that relates the “input” with the “output”. The closer these are, in a correlational sense, the better the fit. Individual correlations are obtained for each of the k variables separately. These magnitudes are the k maximal correlations that measure the “goodness-of-fit” of the k regressions. A correlation of 1 means that the vectors have a perfect fit with the original variable data. In general, as the number of (poor) variables decreases, the average correlation increases and average of correlations of 0.7 or greater provide maps that fit the data well (Bravata *et al.* 2008).

2.3 Experimental setup

The schematic diagram of the experimental setup is shown in Fig. 2. The pilot MBR was equipped with a hollow fiber ultrafiltration (UF) membrane module of ZW-10 (Zenon Environmental Inc., Canada). The cylindrical module was submerged in a 190 L (working volume) drum-tank. The membranes had a nominal pore size of 0.04 µm and a total filtering surface area of 0.93 m². A 2" draft tube, Ø = 235 mm was used to induce the crossflow velocity. The draft-tube was located in the centre of the bioreactor and divided the bioreactor into a riser zone, where the membrane module was submerged in the centre, and a down-comer zone, which was connected by a bottom flow channel and an upper flow channel. Air supply was maintained by coarse air bubble sparging from 4 small holes (Ø = 2 mm) which were located at the bottom of the membrane bundle (Yang *et al.* 2006).

2.4 Operating conditions

The experiments were conducted under ambient conditions in the Sde Boker campus, Ben Gurion University of the Negev, Israel. Domestic wastewater was taken from the mobile houses (Caravans) residential area in Kiryat Sde-Boker, and fed into the bioreactor through a 0.8 mm screen. Initially, the bioreactor was inoculated with the activated sludge collected from the Beer Sheva Municipal Wastewater Treatment Plant.

During the operating period, excess sludge was discharged daily to maintain the concentration of Mixed Liquor Suspended Solids (MLSS) around 6.5 g/L. The average SRT was 30 days. The permeate was intermittently extracted with a suction mode of 5 min and 15 seconds of backwashing. The experiments were manipulated under combined hydraulic conditions with different aeration rates and different permeate rates, according to the scheme of the integrated experimental design. The

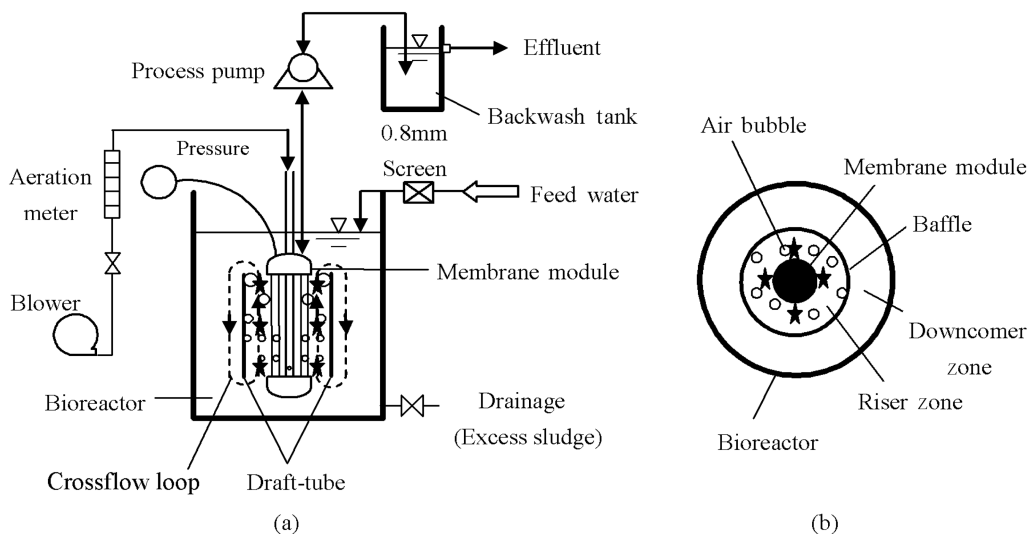


Fig. 2 Schematic diagram of the MBR. (a) Sectional figure ; (b) Above view. ★ indicates velocity measuring points

Table 2 Qualities of influent and effluent (mean \pm standard deviation) and related removal

Parameter, mg/L	Influent	*Effluent	Removal, %
Alkalinity	269 \pm 41	213 \pm 71	21.1
PO ₄ ³⁻ -P	11 \pm 2.0	9.1 \pm 1.8	16.3
DO	3.3 \pm 0.9	----	----
COD	510 \pm 112	106 \pm 54	79.1
BOD ₅	188 \pm 57	6.4 \pm 3.3	96.6
NH ₄ -N	42 \pm 5.4	23 \pm 11	45.0
NO ₃ -N	0.7 \pm 0.5	**8.0 \pm 6.5	---
Total-N	47 \pm 5.3	32 \pm 7.9	31.1

*Effluent qualiy: Turbidity mean value 0.2 NTU

**Nitrate concentration in the effluent (permeate) was higher than that in the Influent, probably due to extra nitrification carried out by *Nitrospira* bacteria on the membrane biofilm

temperature range in the reactor during the operating period was 6.1 to 31.1°C with the mean of 19.5°C. The water qualities of the influent and effluent are shown in Table 2 [COD, BOD₅, NH₄⁺-N, Total-N, PO₄³⁻-P and Alkalinity were analyzed according to the Standard methods (APHA, 1998), NO₃⁻-N was determined with a second-derivative spectroscopy, following by a specific analysis (Ferree and Shannon 2001)].

In order to remove the sludge deposited on the membrane surface (during each experimental stage), at the end of each test, stopping suction, aeration at 3.4 m³/hr without filtration was continued for 24 hrs. Then the next test was conducted. Chemical cleaning with a 750 mg/L sodium hypochlorite solution was carried out after each experimental stage for the membrane permeability recovery.

Filtration performance was evaluated by fouling tendency. Under constant-flux mode, TMP increases over time and (dP/dt) indicates the membrane fouling rate. In order to determine the fouling rate for the conditions tested, a flux-step method was employed (Germain, *et al.* 2005): without backwashing, increased permeate flux step by step with a step duration of 1.5 hours. Between each step, the membrane was backwashed with permeate for 30 min in order to eliminate the reversible fouling built up during one step to be transferred to the next step. The flux-step method was used to determine membrane fouling rate under the combinations between permeate flux and aeration rate (1.7, 2.55, 3.4, 4.25, 5.1 m³/hr) in 2" draft tubes. The permeate fluxes at different temperatures were normalized to 20°C according to Eq. (13) (Bersillon and Thompson 1998)

$$J_{20} = J_t \times \frac{\mu_t}{\mu_{20}} = J_t \cdot e^{-0.0239(T-20)} \quad (6)$$

where J_t is the permeate flux at t time, L/(m².hr); J_{20} is the normalized permeate flux (at 20°C), L/(m².hr); μ_t and μ_{20} is the viscosity of permeate at t time and 20°C, mPa.s; T is the temperature at t time, °C.

The airflow rate was controlled by a rotameter. The filtration flux was monitored using a volumetric method. The TMP was monitored by a digital pressure indicator. The mixed liquor temperature was monitored by a temperature indicator located on the reactor wall. The effluent temperature was detected using a thermometer.

The crossflow velocities were measured by an electromagnetic flow velocity meter (Model 2000, Marsh-McBirney, USA) at 12 measuring sites (Fig. 2), respectively. For each site, the observed flow

velocity was an average of 6 measured values. The final adopted crossflow velocities were the mean values of the observed data.

3. Results and discussion

3.1 MBR performance

According to “traditional” point of view, the use of mathematical modeling and direct observation technique to analyse flux decline is constructive (Lin *et al.* 2008, Jamal Khan *et al.* 2009, Marselina *et al.* 2009, Rodrigues *et al.* 2010) and practical (Zondervan *et al.* 2009). Concerning these aspects, it seems that the tests were conducted within a short period of time without consideration on the change of mixed liquor characteristics due to DO concentration over long term operation (Fig. 3 and

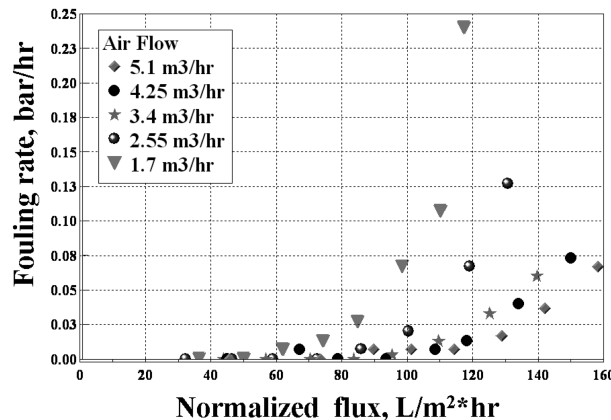


Fig. 3 Fouling rate dP/dt vs. permeate flux J_{20} at different aeration rate in the 2# tube

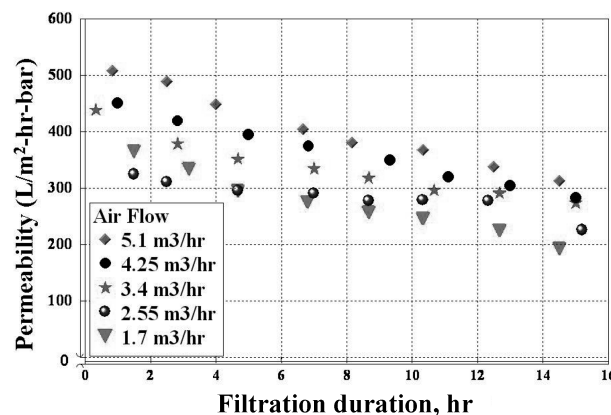


Fig. 4 Permeability (permeate flux J_{20} divided by TMP) vs. filtration duration at different aeration rate in the 2# tube

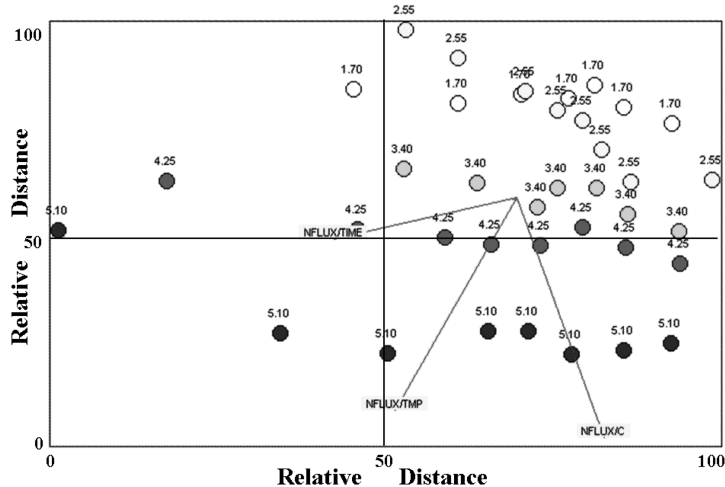


Fig. 5 MDS map, generated by the proposed method (CoPlot): IMBR performance at different aeration rate m^3/hr (2" draft tube, $\varnothing = 235 \text{ mm}$). (Aeration rate: white circles = $1.70 \text{ m}^3/\text{hr}$, yellow circles = $2.55 \text{ m}^3/\text{hr}$, green circles = $3.40 \text{ m}^3/\text{hr}$, red circles = $4.25 \text{ m}^3/\text{hr}$ and blue circles = $5.1 \text{ m}^3/\text{hr}$). The location of each point (test data) was mapped by an algorithm: ‘close’ observations (with a small dissimilarity between them) are close to each other on the map, while ‘far-off’ ones are distant on the map. The number near each point specifies the aeration rate in m^3/hr . The variables are: normalized flux per time NFLUX/TIME, normalized flux per Celsius centigrade NFUX/C, and normalized flux per Trans membrane pressure NFLUX/TMP. Each variable is represented by an arrow, emerging from the centre of gravity of the n points. The direction of each arrow is chosen so that the correlation between the actual values of the variable and their projections on the arrow is maximal. [MDS Statistics: “Coefficient of alienation”, 0.055, Average of Correlations: 0.969 (NFLUX/TIME, 0.94; NFLUX/TMP, 0.99; NFLUX/C, 0.97)]. The “goodness-of-fit” measures (concerning the “Coefficient of alienation” and the variables correlations) is satisfied both for the observations and the variables.

Fig. 4) and the researchers will be advised to conduct further analysis in order to reach the plateau. Concerning MDS analysis of the test results, there is no need to continue the experiments because fouling rate was reduced significantly with the increase of aeration rate at $5.1 \text{ m}^3/\text{hr}$ (Fig. 5 and Table 1) and the results tended to be superior and clearly outlying compare to the other experiments (Tests that were performed with aeration rate less than $3.5 \text{ m}^3/\text{hr}$).

3.2 Discussion

It is being argued in this paper that MDS can be used to present the result graphically, by using the ratio of variables ($\text{output}_o/\text{input}_p$) rather than the original data. The efficient units in a MDS appear in the outer ring or sector of observations in the plot and it is easy to identify over which ratios specific observations are particularly good.

In our case (IMBR) the inputs are: feed temperature [C], test duration [TIME] and trans-membrane pressure and the output is the normalized flux[NFLUX].[The ratios (r_{op}) are: normalized flux per time NFLUX/TIME, normalized flux per Celsius centigrade NFUX/C, and normalized flux per Trans membrane pressure NFLUX/TMP (permeability)].

The higher the ratio (r_{op}) a unit receives, the more efficient the DMU is considered over that specific attribute and it is clearly shown (Fig. 5) that the best IMBR performance is achieved with air flow

of $5.1 \text{ m}^3/\text{hr}$. At high aeration rate of $5.1 \text{ m}^3/\text{hr}$, the normalized flux per time, the normalized flux per Celsius centigrade, and the normalized flux per trans membrane pressure were found to be excellent.

The “goodness-of-fit” of the Coplot technique is assessed by two types of measures: the “coefficient of alienation” Θ and the magnitudes of the v maximal correlations that measure the “goodness-of-fit” of the v regressions.

The smaller the “coefficient of alienation” the better the output and values below 0.15 are considered good. In this case a coefficient of 0.055 is considered as an excellent figure. The “goodness-of-fit” of the v regressions help in deciding whether to eliminate or add variables: Variables that do not fit into the graphical display, namely, have low correlations, and should be removed. The higher the variable’s correlation, the better the variable’s arrow represents common direction and order of the projections of the n points along the axis.

Based on this test case, the correlations of MDS data are excellent: average 0.969 [(NFLUX/TIME, 0.94; NFLUX/TMP, 0.99; NFLUX/C, 0.97)]. The two “goodness-of-fit” measures (“coefficient of alienation” for the first step and three correlations for each one of the variables for the second step) enable the researchers to point out the importance of the aeration rate. According to the experimental data the MDS plot (Fig. 5) is preferable on the flux decline illustration (Fig. 3) and the permeability illustration (Fig. 4): (i) it takes into account temperature, duration time and the Trans-Membrane Pressure (TMP), and; (ii) the new variables clearly show the effect of aeration (experimental points are not adjacent when aeration rate is beyond $3.4 \text{ m}^3/\text{hr}$).

4. Conclusions

This paper makes two important contributions. First, it presents the Coplot technique, a multivariate statistical method that is remarkably robust: handles a wide variety of instances and obtains results competitive with customary methods (fouling rate and permeability). Second, it provides new insights about IMBR performance and air flow, giving a clear view of what needs to be done next. The procedure allows determining the relative technical efficiency (a function of temperature, trans-membrane pressure, normalized permeate flux and filtration duration).

The Coplot technique provides a powerful analytic tool for IMBR analysis. The results indicate that: (i) aeration plays an important role in IMBR performance. At a high aeration rate of $5.1 \text{ m}^3/\text{hr}$, the normalized flux per time, the normalized flux per Celsius centigrade, and the normalized flux per trans membrane pressure were found to be excellent, (ii) implementing the MDS approach with reference to the technical efficiency is consequently useful to characterize performance changes for data classification, clearly illustrates the conflicting influence of membrane fouling and aeration rate and can detect small deviations from expected performance of the system.

Acknowledgments

This work was supported partially by the SMART (Sustainable Management of Available Water Resources with Innovative Technologies) project financed by the Ministry of Science of the German government [Projektantrag zum BMBF-Förderschwerpunkt, Integriertes Wasserressourcen-Management (IWRM)], by The Beracha Foundation, The Stephen and Nancy Grand Water Research Institute, The Technion, Haifa Israel, The Palestinian-Jordanian-Israeli Project (PJIP) (1996), on Membrane

Technology for Secondary Effluent Polishing: From Raw Sewage to Valuable Waters and Other By-Products, and by The Levin Family Foundation, Dayton, Ohio, USA, on Membrane Use for Wastewater Reclamation and the Research Authority of Jerusalem College of Technology (JCT), Israel. The forth auther was supported in part by the Recanati Foundation.

References

- Abegglen, C., Ospelt, M. and Siegrist, H. (2008), "Biological nutrient removal in a small-scale MBR treating household wastewater", *Water Res.*, **42**(1-2), 338-346.
- Adler, N. and Raveh, A. (2008), "Presenting DEA graphically", *Omega*, **36**(5), 715-729.
- Agashichev, S.P. (2009), "Modeling the influence of temperature on gel-enhanced concentration polarization in reverse osmosis", *Desalination*, **236**(1-3), 252-258.
- APHA (1998), *Standard methods for the examination of water and wastewater*, 20th edition, Washington D.C.
- Bersillon, J. and Thompson, M.A. (1998), *In Situ Evaluation and Operation in Water Treatment Membrane Processes*, McGraw-Hill, Madrid.
- Beyer, M., Lohrengel, B. and Nghiem L.D. (2010), "Membrane fouling and chemical cleaning in water recycling applications", *Desalination*, **250**(3), 997-981.
- Bick, A., Plazas, J.P. and Oron, G. (2005), "Immersed membrane bioreactor (IMBR) for treatment of combined domestic and dairy wastewater in an isolated farm", *Water Sci. Technol.*, **51**(10), 327-334.
- Bick, A., Yang, F., Shandalov, S. and Oron, G. (2007), "Data envelopment analysis for assessing optimal operation of an immersed membrane bioreactor equipped with a draft tube for domestic wastewater reclamation", *Desalination*, **204**(1-3), 17-23.
- Bick, A., Plazas, J.P. Yang, F., Hagin, J. and Oron, G. (2009), "Immersed Membrane BioReactor (IMBR) for treatment of combined domestic and dairy wastewater in an isolated farm: an exploratory case study implementing the Facet Analysis (FA)", *Desalination*, **249**, 1217-1222.
- Bottino, A., Capannelli, G., Comite, A., Ferrari, F., Firpo, R. and Venzano, S. (2009), "Membrane technologies for water treatment and agroindustrial sectors", *C. R. Chimie*, **12**(8), 882-888.
- Bravata, D.M., Shojania, K.G., Olkin, I. and Raveh, A. (2008), "CoPlot: A tool for visualizing multivariate data in medicine", *Statist. Med.*, **27**(12), 2234-2247.
- Chae, S.R., Ahn, Y.T., Kang, S.T. and Shin, H.S. (2006), "Mitigated membrane fouling in a vertical submerged membrane bioreactor (VSMBR)", *J. Membrane Sci.*, **280**(1-2), 572-581.
- Chang, C.Y., Chang, J.S., Vigneswaran, S. and Kandasamy, J. (2008), "Pharmaceutical wastewater treatment by membrane bioreactor process – a case study in southern Taiwan", *Desalination*, **234**(1-3), 393-401.
- Charnes, A., Cooper, W.W. and Rhods, H. (1978), "Measuring the efficiency of decision-making units", *Eur. J. Oper. Res.*, **2**(6), 429-444.
- Chen, J.C., Elimelech, M. and Kim, A.S. (2005), "Monte carlo simulation of colloidal membrane filtration: Model development with application to characterization of colloid phase transition", *J. Membrane Sci.*, **255**, 291-305.
- Chen, Y.C., Lien, H.P. and Tzen G. H. (2010), "Measures and evaluation for environment watershed plans using a novel hybrid MCDM model", *Expert Systems with Applications*, **37**(2), 926-938.
- Choi, J.H. and Ng, H.Y. (2008), "Effect of membrane type and material on performance of a submerged membrane bioreactor", *Chemosphere*, **71**(5), 853-859.
- Cicek, N., Suida, M.T., Ginestet, P. and Audi, J.M. (2002), "Impact of soluble organic compounds on permeate flux in an aerobic membrane bioreactor", *J. Envir. Technol.*, **24**(2), 249-256.
- Drews, A., Lee, C.H. and Kraume, M. (2006), "Membrane fouling – a review on the role of EPS", *Desalination*, **200**, 186-188.
- Ferree, M. A. and Shannon, R.D. (2001), "Evaluation of a second derivative uv/visible spectroscopy technique for nitrate and total nitrogen analysis of wastewater samples", *Water Res.*, **35**(1), 327-332.
- Germain, E., Stephenson, T. and Pearce, P. (2005), "Biomass characteristics and membrane aeration: toward a better understanding of membrane fouling in submerged membrane bioreactors (MBRs)", *Biotech. Bioeng.*,

- 90(3), 316-322.
- Gillerman, L., Bick, A., Buriakovskiy, N. and Oron, G. (2006), "Secondary wastewater polishing with ultrafiltration membranes for unrestricted reuse: Fouling and flushing modeling", *Environ. Sci. Technol.*, **40**, 6830-6836.
- Guttman, L. (1968), "A general non-metric technique for finding the smallest space for a configuration of points", *Psychometrica*, **33**(4), 479-506.
- Jamal Khan, S., Visvanathan, C. and Jegatheesan, V. (2009), "Prediction of membrane fouling in MBR systems using empirically estimated specific cake resistance", *Bioresource Tech.*, **100**(23), 6133-6136.
- Jiang, T., Kennedy, M.D., Van der Meer, W.G.J., Vanrolleghem, P.A. and Schippers, J.C. (2003), "The role of blocking and cake filtration in MBR fouling", *Desalination*, **157**(1-3), 335-343.
- Jiang, T., Kennedy, M.D., Yoo, C., Nopens, I., Van der Meer, W., Futselaar, H., Schippers, J.C. and Vanrolleghem, P.A. (2007), "Controlling submicron particle deposition in a side-stream membrane bioreactor: A theoretical hydrodynamic modeling approach incorporating energy consumption", *J. Membrane Sci.*, **297**(1-2), 141-151.
- Joss, A., Keller, E., Alder, A.C., Gobel, A., McArdell, C.S., Ternes, T. and Siegrist, H. (2005), "Removal of pharmaceuticals and fragrances in biological wastewater treatment", *Water Res.*, **39**(14), 3139-3152.
- Joss, A., Zabczynski, S., Gobel, A., Hoffmann, B., Loffler, D., McArdell, S.M., Ternes, T.A., Thomsen, A. and Siegrist, H. (2006), "Biological degradation of pharmaceuticals in municipal wastewater treatment: Proposing a classification scheme", *Water Res.*, **40**(8), 1686-1696.
- Koning, J.D., Karabelas, B.A., Salgot, M. and Schäfer, A. (2008), "Characterization and assessment of water treatment technologies for reuse", *Desalination*, **218**, 92-104.
- Le-Clech, P., Chen, V. and Fane, A.G. (2006), "Fouling in membrane bioreactors used in wastewater treatment", *J. Membrane Sci.*, **284**(1-2), 17-53.
- Leiknes, T. and Ødegaard, H. (2007), "The development of a biofilm membrane bioreactor", *Desalination*, **202**(1-3), 135-143.
- Lesjean, B. and Leiknes, T. (2006), "AMEDEUS and EUROMBRA projects: boosting the development of MBR technologies in Europe", *Desalination*, **200**, 710-711.
- Lin, S., Hung, C. and Juang, R. (2008), "Applicability of the exponential time dependence of flux decline during dead-end ultrafiltration of binary protein solutions", *Chem. Eng. J.*, **145**(2), 211-217.
- Lipshitz, G. and Raveh, A. (1994), "Applications of the CoPlot method in the study of socioeconomic differences among cities: A basis for a differential development policy", *Urban Studies*, **31**, 123-135.
- Macedonio, F., Di Profio, G., Curcio, E. and Drioli, E. (2006), "Integrated membrane systems for seawater desalination", *Desalination*, **200**, 612-614.
- Marselina, Y., Lifia, A., Le-Clech, R., Stuetz, R.M. and Chen, V. (2009), "Characterisation of membrane fouling deposition and removal by direct observation technique", *J. Membrane Sci.*, **341**, 163-161.
- Matos, C.T., Fortunato, R., Velizarov, S., Reis, M.A.M. and Crespo, J.O. (2008), "Removal of mono-valent oxyanions from water in an ion exchange membrane bioreactor: Influence of membrane permselectivity", *Water Res.*, **42**(6-7), 1785-1795.
- McAdam, E.J., Judd, S.J., Cartmell, E. and Jefferson, B. (2007), "Influence of substrate on fouling in anoxic immersed membrane bioreactors", *Water Res.*, **41**(17), 3859-3867.
- Mosqueda-Jimenez, D.B. and Huck, P.M. (2006), "Characterization of membrane foulants in drinking water treatment", *Desalination*, **198**(1-3), 173-182.
- Oehmen, A., Lemos, P.C., Carvalho, G., Yuan, Z., Keller, J., Blackall, L.L. and Reis, M.A.M. (2007), "Advances in enhanced biological phosphorus removal: From micro to macro scale", *Water Res.*, **41**(11), 2271-2300.
- Oron, G., Gillerman, L., Buriakovskiy, N., Bick, A., Gargir, M., Dolan, Y., Manor, Y., Katz, L. and Hagin, J. (2008), "Membrane technology for advanced wastewater reclamation for sustainable agriculture production", *Desalination*, **218**(1-3), 170-180.
- Petala, M.D. and Zouboulis, A.I. (2006), "Vibratory shear enhanced processing membrane filtration applied for the removal of natural organic matter from surface waters", *J. Membrane Sci.*, **269**(1-2), 1-14.
- Pollice, A., Brookes, A., Jefferson, B. and Judd, S. (2005), "Sub-critical flux fouling in membrane bioreactors recent literature", *Desalination*, **174**(3), 221-230.
- Qin, J.-J., Wai, M.N., Tao, G., Kekre, K.A. and Seah, H. (2007), "Membrane bioreactor study for reclamation of

- mixed sewage mostly from industrial sources”, *Sep. Purif. Technol.*, **53**(3), 296-300.
- Raveh, A. (2000), “CoPlot: A Graphic display method for geometrical representations of MCDM”, *Eur. J. Oper. Res.*, **125**(3), 670-678.
- Rieger, L., Thomann, M., Gujer, W. and Siegrist, H. (2005), “Quantifying the uncertainty of on-line sensors at WWTPs during field operation”, *Water Res.*, **39**(20), 5162-5174.
- Rodrigues, F., Cavaco Morao, A.L., de Pinho, M.N. and Geraldes, V. (2010), “On the prediction of permeate flux for nanofiltration of concentrated aqueous solutions with thin-film composite polyamide membranes”, *J. Membrane Sci.*, **346**, 1-7.
- Rossi, L., Krejci, V., Rauch, W., Kreikenbaum, S., Fankhauser, R. and Gujer, W. (2005), “Stochastic modeling of total suspended solids (TSS) in urban areas during rain events”, *Water Res.*, **39**(17), 4188-4196.
- Salgot, M. (2008), “Water reclamation, recycling and reuse: implementation issues”, *Desalination*, **218**(1-3), 190-197.
- Schilli, C., Lischeid, G. and Rinklebe, J. (2010), “Which processes prevail?: Analyzing long-term soil solution monitoring data using nonlinear statistics”, *Geoderma*, **158**(3-4), 412-420.
- Shon, H.K., Vigneswaran, S. and Snyder, S.A. (2006), “Effluent organic matter (EfOM) in wastewater: constituents, effects and treatment”, *J. Envir. Sci. Technol.*, **36**(4), 327-374.
- Shon, H.K., Vigneswaran, S., Kandasamy, J. and Shim, W.G. (2008), “Ultrafiltration of wastewater with pretreatment: evaluation of flux decline models”, *Desalination*, **231**(1-3), 332-339.
- Song, L., Chen, K.L., Ong, S.L. and Ng, W.J. (2004), “A new normalization method for determination of colloidal fouling potential in membrane processes”, *J. Colloid Interface Sci.*, **271**(2), 426-433.
- Sonicki, Z., Cvitkovic, A., Edwards, K.L., Miletic-Medved, M., Cvoriscec, D., Babus, V. and Jelakovic, B. (2009), “Visual Assessment of Endemic Nephropathy Markers Relationship”, *Stud. Health Technol. Inform.*, **150**, 836-840.
- Sophonsiri, C. and Morgenroth, E. (2004), “Chemical composition associated with different particle size fractions in municipal, industrial, and agricultural wastewaters”, *Chemosphere*, **55**(5), 691-703.
- Sridang, P.C., Anthony Pottier, A., Wisniewski, C. and Grasnick, A. (2008), “Performance and microbial surveying in submerged membrane bioreactor for seafood processing wastewater treatment”, *J. Membrane Sci.*, **317**(1-2), 43-49.
- Tan, T.W. and Ng, H.Y. (2008), “Influence of mixed liquor recycle ratio and dissolved oxygen on performance of pre-denitrification submerged membrane bioreactors”, *Water Res.*, **42**(4-5), 1122-1132.
- Wenbo, Y., Cicek, N. and Ilg, J. (2006), “State-of-the-art of membrane bioreactors: Worldwide research and commercial applications in North America”, *J. Membrane Sci.*, **270**(1-2), 201-211.
- Winward, G.P., Avery, L.M., Frazer-Williams, R.F., Pidou, M., Jeffrey, P., Stephenson, T. and Jefferson, B. (2008), “A study of the microbial quality of grey water and an evaluation of treatment technologies for reuse”, *Ecol. Eng.*, **32**(2), 187-197.
- Yang, F., Bick, A., Shandalov, S. and Oron, G. (2006), “Optimal performance of an immersed membrane bioreactor equipped with a draft tube for domestic wastewater reclamation”, *Water Sci. Technol.*, **54**(10), 155-162.
- Yang, F., Wang, Y., Bick, A., Brenner, A., Ben-David, E. and Oron, G. (2009), “A long-term application of a pilot airlift membrane bioreactor for domestic wastewater treatment”, *Desal. Water Treatment*, **4**, 212-217.
- Zondervan, E., Bakker, S., Nederlof, M. and Roffel, B. (2009), “Taking green anti-fouling strategies in dead-end ultrafiltration to the next level”, *Chem. Eng. Res. Des.*, **87**(12), 1589-1595.

ED

Nomenclature

d	distance
dP	differential membrane pressure change
dt	differential time change
D	column standard deviations

J	permeate flux, L/(m ² .hr)
J_{20}	normalized permeate flux (at 20°C), L/(m ² -hr)
n	number of test records
NFLUX	normalized flux
NFLUX/C	normalized flux per Celsius centigrade
NFLUX/TIME	normalized flux per time
NFLUX/TMP	normalized flux per Trans-membrane pressure
r	ratio between outputs of the system and inputs
S	sum of absolute deviations
T	temperature, °C
TMP	Trans-membrane Pressure
v	variables number
\bar{Y}	matrix average data
Y	matrix data
Z	normalized matrix data

Greek letters

μ_{ca}	variable used for computation of the “coefficient of alienation”, dimensionless
μ	viscosity of permeate, mPa.s
μ_{20}	viscosity of permeate at 20°C, mPa.s
Θ	“coefficient of alienation”, dimensionless

Subscripts

i	test record observation index
j	test record observation index
k	test record observation index
l	test record observation index
m	test record observation index
o	variable index
p	variable index
t	time